QUANTUM THEORY OF SASE-FEL WITH DISCRETE SPECTRUM*

R. Bonifacio, INFN-MI, Milan, Italy and Universidade Federal de Alagoas, Maceiò, Brazil
N. Piovella#, INFN-MI, Milan and Università degli Studi di Milano, Milan, Italy
G.R.M. Robb, Department of Physics, University of Strathclyde, Glasgow, G4 0NG, Scotland, UK

Abstract

We present a proof of principle of the novel regime of quantum SASE with high temporal coherence and discrete spectrum. Using a self-consistent system of Schroedinger-Maxwell equations with propagation effects, we show that the dynamics of the system are determined by a properly defined "quantum Fel-parameter", $\bar{\rho}$, which represents the ratio between the classical momentum spread in the high gain regime and the one photon recoil momentum $\hbar k$. In the limit $\bar{\rho} >> 1$ the quantum model reproduces the classical SASE regime with random spiking behavior and broad spectrum. In this limit we show that the equation for the quantum Wigner function reduces to the classical Vlasov equation. In the opposite limit, $\bar{\rho} < 1$, we demonstrate "quantum purification" of SASE: the classical chaotic spiking behaviour disappears and the spectrum becomes a series of discrete very narrow lines which correspond to transitions between discrete momentum eigenstates, resulting in high temporal coherence.

INTRODUCTION

The Self Amplified Superradiant Emission (SASE) regime for a free-electron laser (FEL) is made up of three basic ingredients: high-gain, propagation or 'slippage' effects and start-up from noise [1]. The classical steady-state high-gain regime of FELs, with universal scaling and the introduction of the ρ-BPN parameter, was analyzed in [2], where the possibility of operating an FEL in the SASE regime was suggested. Other treatments assume that SASE is just steady state instability starting from noise [3,4]. This approach does not give the correct temporal structure and spectrum of SASE radiation as described in [1].

In [5-7] it was shown that due to propagation there exists not only the steady-state instability of [2], but also a Superradiant instability, with peak intensity proportional to n^2, where n is the electron density. This Superradiant instability, entirely due to slippage, is the heart of SASE, so that all the treatments which claim to describe SASE without this propagation induced instability are fundamentally incorrect [3,4].

As shown in [1], a SASE FEL radiates a random series of Superradiant spikes because, approximately speaking, the electron bunch contains many cooperation lengths which radiate randomly and independently from one another. The final result is an almost chaotic temporal pulse structure with a broad spectral width. The number of spikes in the high-gain regime corresponds approximately to the number of cooperation lengths in the electron bunch. Hence, classical SASE has one drawback with regard to its application as a useful source of short-wavelength coherent light: at short wavelengths many cooperation lengths lie within the electron bunch. This implies a quasi-chaotic temporal structure of the radiation pulse and a consequent wide spectrum.

In this paper we propose a novel method for producing coherent short wavelength radiation with SASE by adding new features to a previous treatment [8]. We introduce a quantum description of SASE which depends on the dimensionless "quantum FEL parameter", $\bar{\rho}$, which is defined in terms of the classical ρ-BPN parameter as:

$$\bar{\rho} = \left(\frac{mc\gamma_r}{\hbar k}\right)\rho \,. \tag{1}$$

$\bar{\rho}$ represents the ratio between the classical momentum spread at saturation and the one photon electron recoil. We show that when $\bar{\rho} >> 1$ the SASE FEL behaves classically, i.e. in agreement with the SASE classical model. However, when $\bar{\rho} \leq 1$, we obtain a quantum regime with features completely different from those of the classical regime and to which we shall refer as Quantum SASE. A surprising feature of this regime is the phenomenon of "quantum purification", in which the chaotic spectrum of classical SASE is replaced by a completely different coherent spectrum. More specifically, in the quantum regime one has a set of discrete narrow lines equally spaced due to transition between discrete momentum states. Increasing $\bar{\rho}$ the distance between the lines decreases and their width increases. The classical continuous noisy spectrum is recovered when, increasing $\bar{\rho}$, the lines overlap.

In this paper we describe Quantum SASE by extending Preparata's model [9] to include propagation effects via a multiple scaling method used in classical FEL theory [10]. This allows us to easily take into account the existence of two different space scales: the variation of the electron distribution on the scale of the radiation wavelength (describing the bunching) and the variation of the field envelope on the much longer scale of the cooperation length.

*Work supported by INFN, Italy
#nicola.piovella@mi.infn.it

QUANTUM FEL MODEL

The Quantum FEL (QFEL) is described by the following equations for the dimensionless radiation amplitude and the "matter wave" $\Psi(\theta, \bar{z}, z_1)$:

$$i\frac{\partial \Psi}{\partial \bar{z}} = -\frac{1}{2\bar{\rho}}\frac{\partial^2 \Psi}{\partial \theta^2} - i\bar{\rho}\left[A(\bar{z}, z_1)e^{i\theta} - c.c.\right]\Psi \tag{2}$$

$$\frac{\partial A}{\partial \bar{z}} + \frac{\partial A}{\partial z_1} = \frac{1}{2\pi}\int_0^{2\pi}\left|\Psi(\theta, \bar{z}, z_1)\right|^2 e^{-i\theta} d\theta + i\delta A \tag{3}$$

The notations are well known [1,8]. In particular, $\bar{z}$ is the coordinate along the wiggler in units of the gain length, $L_g = \lambda_w / 4\pi\rho$, and z_1 is the electron coordinate along the bunch, in units of the cooperation length, $L_c = \lambda_r / 4\pi\rho$. A is the adimensional field amplitude defined so that $\bar{\rho}|A|^2$ is the ratio between the photon density and the electron density, and δ is the normalized detuning.

From Eqs. (2)-(3) one can show that the dimensionless density profile $I_0(z_1) = \int_0^{2\pi}|\Psi|^2 d\theta$ is independent of $\bar{z}$. This means that the space distribution of the particles does not change appreciably on the slow scale z_1 during the interaction with the radiation field. The QFEL equations (2) and (3) depend only on the quantum FEL parameter, $\bar{\rho}$.

The classical limit of the QFEL can be explicitly shown as follows. Eq.(1) can be transformed into an equation for the Wigner function [11,12]

$$\begin{aligned}&\frac{\partial W(\theta,\bar{p},\bar{z},z_1)}{\partial \bar{z}} + \bar{p}\frac{\partial W(\theta,\bar{p},\bar{z},z_1)}{\partial \theta} - \left(Ae^{i\theta} + A^*e^{-i\theta}\right)\times \\ &\bar{\rho}\left[W\left(\theta, \bar{p}+\frac{1}{2\bar{\rho}}, \bar{z}, z_1\right) - W\left(\theta, \bar{p}-\frac{1}{2\bar{\rho}}, \bar{z}, z_1\right)\right] = 0\end{aligned} \tag{4}$$

whereas Eq.(2) becomes

$$\frac{\partial A}{\partial \bar{z}} + \frac{\partial A}{\partial z_1} = \frac{1}{2\pi}\int_{-\infty}^{\infty} d\bar{p}\int_0^{2\pi} d\theta W(\theta, \bar{p}, z_1, \bar{z})e^{-i\theta} + i\delta A \tag{5}$$

where $\bar{p} = mc(\gamma - \gamma_0)/\hbar k\bar{\rho}$. Note that the quantum momentum shift of the Wigner function, $1/2\bar{\rho}$, in dimensional units, would be $\hbar k/2$. In the right hand side of Eq.(4), the second line becomes $\frac{\partial W}{\partial \bar{p}}$ in the limit $\bar{\rho} \to \infty$. Hence, for large values of $\bar{\rho}$, Eq. (4), which is equivalent to Eq.(2), reduces to the classical Vlasov equation:

$$\frac{\partial W}{\partial \bar{z}} + \bar{p}\frac{\partial W}{\partial \theta} - \left(Ae^{i\theta} + A^*e^{-i\theta}\right)\frac{\partial W}{\partial \bar{p}} = 0 \tag{6}$$

Eqs. (4) and (5) provide the description of the QFEL model in terms of the Wigner function, whereas Eqs. (5) and (6) are equivalent to the classical FEL model. Note that Eqs. (5) and (6) do not depend explicitly on $\bar{\rho}$, as must be the case in the classical model with universal scaling [2]. We briefly mention that Eq. (4) for the Wigner function has a broader validity than the Schroedinger equation (2), because it can also describe a statistical mixture of states which cannot be represented by a wavefunction but rather by a density operator.

Eqs.(2) and (3) are conveniently solved in the momentum representation. Assuming that $\Psi(\theta, z_1, \bar{z})$ is a periodic function of θ, it can be written as a Fourier series of momentum eigenstates $e^{in\theta}$:

$$\psi(\theta, z_1, \bar{z}) = \frac{1}{\sqrt{2\pi}}\sum_n c_n(z_1, \bar{z})e^{in(\theta+\delta\bar{z})} \tag{7}$$

so inserting Eq. (7) into Eqs. (2) and (3), we obtain

$$\frac{\partial c_n}{\partial \bar{z}} = -iE_n c_n - \bar{\rho}(Ac_{n-1} - A^* c_{n+1}) \tag{8}$$

$$\frac{\partial A}{\partial \bar{z}} + \frac{\partial A}{\partial z_1} = \sum_{n=-\infty} c_n c^*_{n-1} = b \tag{9}$$

where $E_n = \frac{n^2}{2\bar{\rho}} + \delta n$. Eqs. (8) and (9) are the discrete QFEL model. They are our working equations and their numerical analysis will be discussed in the following section. Note that, from Eq. (7), it follows that $|c_n|^2$ is the probability that an electron has momentum $n\hbar k$. The RHS of Eq.(9) is the quantum expression for the bunching parameter, b, which requires a coherent superposition of different momentum states.

LINEAR ANALYSIS

The stability analysis of Eqs. (8) and (9) has been carried out in [12,13] in the steady state limit. We assume that the system is in an equilibrium state with no field, $A = 0$, and all the electrons are in the state n, with $c_n = 1$ and $c_m = 0$ for all $m \neq n$. Looking for solutions of the linearized equations of the form $e^{i\lambda\bar{z}}$, one obtains the quantum dispersion relation

$$(\lambda - \Delta_n)\left(\lambda^2 - \frac{1}{4\bar{\rho}^2}\right) + 1 = 0 \tag{10}$$

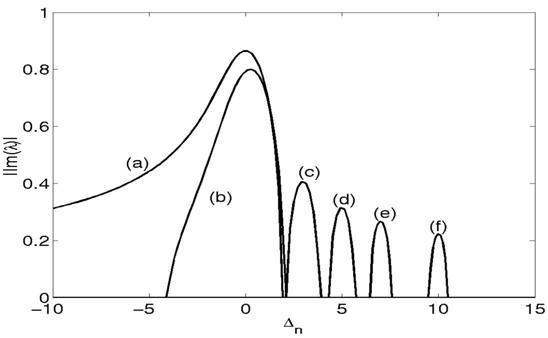

Figure 1: Imaginary part of the unstable root of the cubic equation (13) vs Δ_n, for $1/2\bar{\rho} = 0$.(a), 0.5, (b), 3, (c), 5, (d), 7, (e) and 10, (f).

where $\Delta_n = \delta + n/\bar{\rho}$. The system is unstable when the dispersion relation (10) has complex roots. Notice that this dispersion relation coincides with that of a classical FEL with an initial energy spread with a square distribution and width $1/\bar{\rho}$ [6], which, in dimensional units, becomes $\hbar k$. In Fig.1 we plot the imaginary part of λ as a function of Δ_n for different values of $\bar{\rho}$. The classical limit is obtained for $\bar{\rho} >> 1$ (see Fig.1a).

When $\bar{\rho} \leq 1$ (Fig.1b-f), the resonance moves from $\Delta_n = 0$ to $\Delta_n = 1/2\bar{\rho}$ (in dimensional units $mc(\gamma_0 - \gamma_r) = \hbar k/2$ [14]), with peak value $\mathrm{Im}\,\lambda = \sqrt{\bar{\rho}}$ and full width on δ equal to $4\sqrt{\bar{\rho}}$ (in dimensional units $4\hbar k \bar{\rho}^{3/2}$). However, one can also plot the solution of Eq.(10), for fixed $\bar{\rho}$, as a function of the real detuning δ (see Fig.2). One obtains discrete lines (as in a cavity) centered on $\delta = (1-2n)/2\bar{\rho}$ equally spaced by $1/\bar{\rho}$, whose width is $4\sqrt{\bar{\rho}}$. Eventually, the classical limit with a broad, continuous gain spectrum occurs when the frequency separation, $1/\bar{\rho}$, becomes smaller than the width $4\sqrt{\bar{\rho}}$ of each gain region i.e. $1/\bar{\rho} < 4\sqrt{\bar{\rho}}$ or $\bar{\rho} > 0.4$ (see Fig 2(c)). The physical reason for these discrete frequencies is that in the quantum regime the electron recoils by $\hbar k$, so that electrons undergo a transition from an energy $E_n \propto p^2 \propto n^2$, to the state with energy $E_{n-1} \propto (n-1)^2$. Hence, the transition frequency varies as $(n-1)^2 - n^2 = 1-2n$, as above.

As discussed in [12] for $\bar{\rho} >> 1$ the electrons have almost the same probability of transition from the momentum state $n \to n \pm 1$ (i.e. $|c_{n+1}|^2 \approx |c_{n-1}|^2$), absorbing or emitting a photon. On the contrary, in the case $\bar{\rho} \leq 1$, $|c_{n+1}|^2 << |c_{n-1}|^2$, i.e. the particles can only emit a photon with transition $n \to n-1$, behaving approximately as a two level system [8] described by the so-called Maxwell-Bloch equations [15].

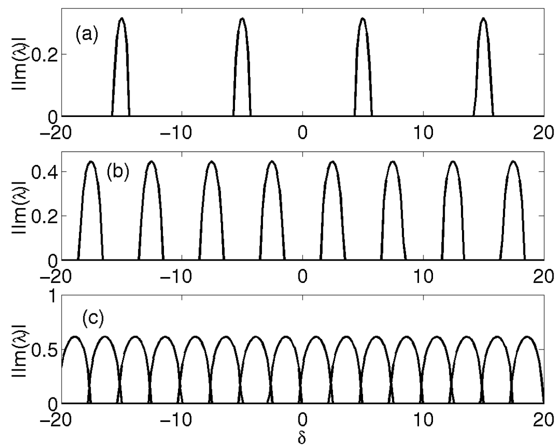

Figure 2: Imaginary part of the unstable root of the cubic equation (13) vs. δ for (a) $\bar{\rho} = 0.1$, (b) $\bar{\rho} = 0.2$, and (c) $\bar{\rho} = 0.4$. The total width of each line is $4\sqrt{\bar{\rho}}$ and the line separation is $1/\bar{\rho}$ centered on $\delta = (1-2n)/2\bar{\rho}$. Continuous limit when $4\sqrt{\bar{\rho}} = 1/\bar{\rho}$, $(\bar{\rho} = 0.4)$

One can show [8] that, in the quantum limit $\bar{\rho} < 1$, one has a quantum gain length, $L_g' = \lambda_w/(4\pi\rho\sqrt{\bar{\rho}})$, and a quantum cooperation length, $L_c' = \lambda_r/(4\pi\rho\sqrt{\bar{\rho}})$, larger by a factor $1/\sqrt{\bar{\rho}}$ than the classical one [1]. This can be easily seen by defining a *universal quantum scaling* as follows: In Eq.(8) and (9) perform the transformation $\bar{z} \to \sqrt{\bar{\rho}}\bar{z}$, $z_1 \to \sqrt{\bar{\rho}} z_1$, $A \to \sqrt{\bar{\rho}} A$, $E_n \to E_n/\sqrt{\bar{\rho}}$. The transformed equation will not contain the coefficient $\bar{\rho}$ in the RHS of Eq.(8), so that the solution will be independent of $\bar{\rho}$. In particular, $\bar{\rho}|A|^2$ (i.e., the photon number per particle) will be invariant and of the order of unity (see Fig.3).

NUMERICAL RESULTS

We now show that the discrete gain spectrum of the quantum regime shown in Fig.2, can give rise to "quantum purification" of the SASE spectrum. Fig. 3 shows a numerical simulation of the QFEL model Eq.(8) and (9).

The simulation assumes all electrons are initially in the momentum state n=0. The initial conditions for all the simulations are therefore $A(z_1, \bar{z}) = 0$, $c_{-1}(z_1, \bar{z} = 0) = b_0 e^{i\phi(z_1)}$ and, $c_0(z_1, \bar{z}) = \sqrt{1 - b_0^2}$ where $b_0 = 0.01$ and

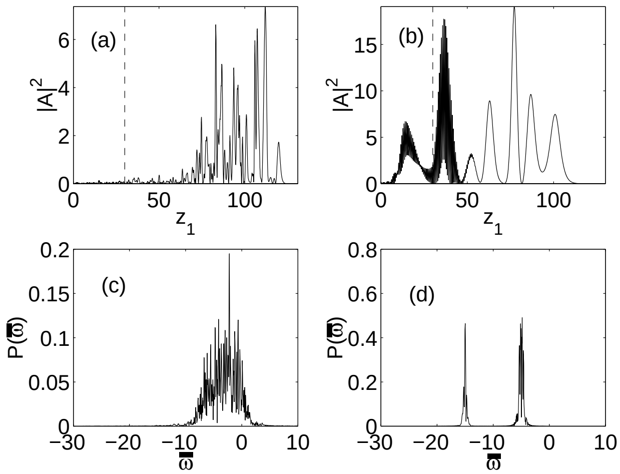

Figure 3: Numerical solutions of Eq. (8) and (9), for $\delta = 0$, in the classical ($\bar{\rho} = 5$) (a, c) and quantum regimes $\bar{\rho} = 0.1$ (b, d) for $\bar{z} = 100$: Graphs (a) and (b) show the scaled intensity and Graphs (c) and (d) show the corresponding scaled power spectra. The dotted line in (a) and (b) mark the front edge of the electron pulse $z_1 = 30$. The frequency shift in (d) is in agreement with that predicted from Fig. 2(a).

$\phi(z_1)$ is a randomly fluctuating phase with values in the range $(0, 2\pi)$. Fig. 3(a) and (b) show the field intensity as a function of z_1 at $\bar{z} = 100$ for the classical and quantum regimes respectively. Fig 3(c) and (d) show the corresponding classical and quantum power spectra of the radiated field versus $\bar{\omega} = (\omega' - \omega)/(2\rho\omega)$, where ω is the resonance (spontaneous emission) frequency. It can be seen that there is a dramatic difference between the classical evolution (Figs 3(a,c)) and the quantum evolution (Figs 3(b,d)). The temporal structure in the classical limit (Fig. 3(a)) is almost chaotic, with a broad spectrum. In contrast, the temporal behaviour in the quantum limit (Fig. 3(b)) shows a purification of the initially noisy evolution, and the corresponding spectrum is composed by narrow lines, in agreement with the linear analysis reported in Fig.2(a).

The frequency position seen in Fig. 3(d) is in agreement with that predicted by linear theory (see Fig.2(a)). Note that the line separation $1/\bar{\rho}$ corresponds in real units to the relativistic recoil frequency $(2\hbar k^2)/(\gamma m)$. The LHS of Fig.3(b) is the unresolved beat between the two frequencies of Fig.3(d). For small values of $\bar{z}$ only the frequency with smaller $\bar{\omega}$ appears. Increasing $\bar{z}$ other lines at distance $1/\bar{\rho}$ will appear.

The reason for quantum purification of the SASE spectrum is as follows : As remarked earlier, in Fig. 1 and 2, the gain bandwidth decreases as $\sqrt{\bar{\rho}}$ and the cooperation length is longer by a factor $\sqrt{\bar{\rho}}$. Hence, one can understand that in quantum SASE, $\bar{\rho} << 1$, the system radiates coherently as if the startup of the FEL interaction is initiated by a coherent bunching or a coherent seed.

CONCLUSIONS

In conclusion, in this paper we have given a proof of principle of the novel regime of Quantum SASE, with dynamical properties very different from "normal" classical SASE. In particular, quantum SASE predicts quantum purification of the temporal structure and spectrum, which becomes a series of discrete narrow lines. We demonstrate that the classical continuous and broad spectrum is obtained when $\bar{\rho}$ is increased so that the distance between the lines, $1/\bar{\rho}$, decreases and their width, $4\sqrt{\bar{\rho}}$, increases until they overlap for $\bar{\rho} \geq 0.4$. The possibility of experimental observation of this quantum regime with a laser wiggler has been presented in [16] and is under further investigation, details of which will be discussed elsewhere [17].

REFERENCES

[1] R. Bonifacio, L. De Salvo, P. Pierini, N. Piovella, and C. Pellegrini, Phys. Rev. Lett. 73 (1994) 70.
[2] R. Bonifacio, C. Pellegrini and L, Narducci, Opt. Commun. 50 (1984) 373.
[3] K.J.Kim, Phys. Rev. Lett. 57 (1986) 1871.
[4] J.M. Wang and L.H. Yu, NIM A 250 (1986) 396.
[5] R. Bonifacio, B. W. J. McNeil, and P. Pierini, Phys. Rev. A 40 (1989) 4467.
[6] R. Bonifacio, F. Casagrande, G. Cerchioni, L. De Salvo Souza, P. Pierini & N. Piovella, Rivista del Nuovo Cimento vol. 13, No. 9 (1990).
[7] R. Bonifacio, C. Maroli and N. Piovella, Opt. Commun. 68 (1988) 369.
[8] R. Bonifacio, N. Piovella, G.R.M. Robb, NIM A 543 (2005) 645.
[9] G. Preparata, Phys. Rev.A 38 (1988) 233.
[10] G.T. Moore and M.O. Scully, Phys. Rev.A 21 (1980) 21.
[11] R. Bonifacio, M. Cola, N. Piovella, and G.R.M.Robb, Europhys. Lett. 69 (2005) 55.
[12] R. Bonifacio, N. Piovella, G.R.M. Robb, and M.M. Cola, Opt. Commun. 252 (2005) 381.
[13] N. Piovella, M. Gatelli, R. Bonifacio, Opt. Commun. 194 (2001) 167.
[14] A. Friedman, A. Gover, G. Kurizki, S. Ruschin, A. Yarin, Rev. Mod. Opt., 60 (1988) 471.
[15] F.T.Arecchi, R.Bonifacio, IEEE, Quantum Elect. 1 (1965) 169. [15] R. Bonifacio, NIM A 546 (2005) 634.
[16] R. Bonifacio, NIM A 546 (2005) 634
[17] R. Bonifacio, M. Ferrario, N. Piovella, L. Serafini, G.R.M. Robb, in this proceedings.